

# Stable Hydrogen Evolution from CdS-Modified CuGaSe<sub>2</sub> Photoelectrode under Visible-Light Irradiation

Makoto Moriya, Tsutomu Minegishi, Hiromu Kumagai, Masao Katayama, Jun Kubota, and Kazunari Domen\*

Department of Chemical System Engineering, The University of Tokyo, 7-3-1 Hongo, Bunkyo-ku, Tokyo 113-8656, Japan

## S Supporting Information

**ABSTRACT:** The photoelectrochemical properties of CuGaSe<sub>2</sub> modified by deposition of a thin CdS layer were investigated. The CdS layer formed a p–n junction on the surface of the electrode, improving its photoelectrochemical properties. There was an optimal CdS thickness because of the balance between the charge separation effect and light absorption by CdS. CdS-deposited CuGaSe<sub>2</sub> showed high stability under the observed reaction conditions and evolved hydrogen continuously for more than 10 days.

Fossil resources such as petroleum, coal, and natural gas are essential fuels supporting the human energy society and they are also converted to indispensable bulk chemicals such as ammonia for fertilizers in food production. However, they are reasonably predicted to be exhausted in the future, and replacement of fossil fuels by renewable energy resources is unavoidable. Hydrogen is regarded as a next-generation energy carrier if it is produced from renewable energy sources. Photoelectrochemical (PEC) water splitting is one possible means of generating hydrogen in an environmentally friendly manner because it requires only semiconductor electrodes, water, and sunlight. To utilize solar energy efficiently, a photoelectrode should meet at least three requirements: an appropriate band gap for sunlight absorption, suitable band positions for water reduction/oxidation, and stability under the required reaction conditions. Many semiconductor materials and a variety of configurations have been surveyed,<sup>1</sup> but satisfying performance has not yet been obtained in a practical manner.

CuGaSe<sub>2</sub> (CGSe) is frequently reported to be a p-type semiconductor and has an absorption edge near 750 nm.<sup>2</sup> Marsen et al.<sup>3</sup> reported that CGSe can function as a photocathode. In that report, the photocurrent of CGSe was 10.6 mA/cm<sup>2</sup> at –0.9 V vs SCE (–0.66 V vs RHE) in a strongly acidic solution. The onset potential of the photocurrent was +0.136 V vs RHE. However, no surface modification was performed, and the onset potential of the photocurrent was relatively low. On the other hand, Yokoyama et al.<sup>4</sup> reported that CdS modification of a Cu(In,Ga)Se<sub>2</sub> photocathode by chemical bath deposition (CBD) clearly increased the photocurrent and onset potential. It has been reported that CdS deposited on Cu(In,Ga)Se<sub>2</sub> by CBD forms a high-quality p–n junction<sup>5</sup> and that enhancement of the charge separation by the formation of this p–n junction results in increased photo-

current and onset potential. In this study, CBD was used to deposit CdS on a CGSe electrode, and the effects of this surface modification on the PEC properties of the electrode were investigated.

CGSe thin films with a thickness of ~1 μm were prepared by coevaporation on Mo-coated soda lime glass plates.<sup>6,7</sup> CdS layers were formed on the prepared CGSe films by CBD. We note that approximately 40, 80, and 150 nm thick CdS layers were formed by CBD for 1, 3, and 10 min, respectively. Pt was photoelectrochemically deposited on the electrodes as a hydrogen evolution promoter prior to the PEC measurements.<sup>4,6–9</sup> The detailed sample preparation methods and experimental conditions for the PEC measurements are shown in the Supporting Information (SI). The prepared samples were analyzed using X-ray diffraction (XRD) (RINT-Ultima3, Rigaku), UV–visible diffuse reflection spectroscopy (UN–vis) (V-670DS, JASCO), photoelectron spectroscopy in air (PESA) (AC-3, Riken Keiki), scanning electron microscopy (SEM) (S-4700, Hitachi), and X-ray photoelectron spectroscopy (XPS) (JPS-90SX, JEOL). The XRD pattern corresponded to that of CuGaSe<sub>2</sub>.<sup>10</sup> The results of sample analysis are shown in the SI. UV–vis and PESA measurements revealed that the band gap of 1.7 eV for CGSe, with valence-band maximum (VBM) and conduction-band minimum (CBM) potentials of –0.8 and +0.9 V vs NHE, respectively. From the declared VBM and CBM potentials estimated using PESA, the band structure of CGSe is suitable for H<sub>2</sub> evolution.

In the PEC characterization, the prepared CGSe electrode generated a photocathodic current, indicating it to be a p-type material. The photocurrent of the electrodes was increased significantly by the deposition of Pt, which acted as a hydrogen evolution promoter. Figure 1 shows the current–potential (*I*–*E*) curves for a Pt-loaded CGSe<sub>2</sub> (Pt/CGSe) electrode and a CGSe electrode with both Pt and CdS modification (Pt/CdS/CGSe). The photocurrent density and onset potential were clearly increased by CdS deposition for 1 min. Because CdS is an n-type semiconductor, the CdS layer and the CGSe<sub>2</sub> formed a p–n junction. The thickness of the depletion layer at the p–n junction was calculated to be of submicrometer order in the CGSe and CdS layers, and a carrier concentration of 10<sup>17</sup> cm<sup>–3</sup> was estimated from a Mott–Schottky plot. Under these conditions, the thin CdS layer was completely covered by the depletion layer, resulting in cathodic polarization, which thickened the depletion layer and blocked the diffusion of

Received: December 28, 2012

Published: February 25, 2013

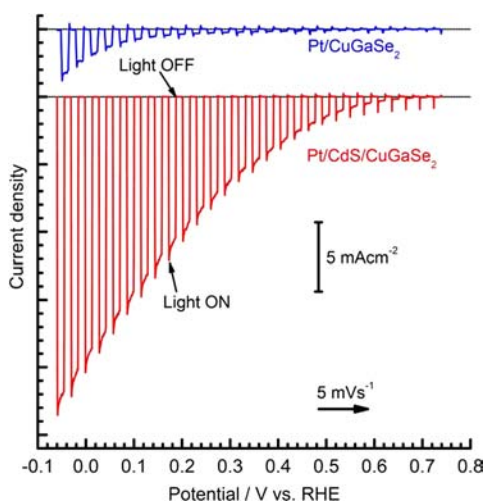


**Figure 1.** Current–potential curves for Pt/CGSe and Pt/CdS/CGSe electrodes [0.1 M Na<sub>2</sub>SO<sub>4</sub>(aq), pH 9, 300 W Xe lamp, 5 mV s<sup>-1</sup>].

holes to the solid–liquid interface as a result of the deeper VBM of CdS compared with CGSe. The modulation of the band diagram around the solid–liquid interface caused by the introduction of the CdS layer resulted in the increased photocurrent and onset potential.

To clarify the role of the CdS layer, the effects of CBD time on the PEC properties of Pt/CdS/CGSe were investigated. Figure 2 shows *I*–*E* curves for Pt/CdS/CGSe electrodes

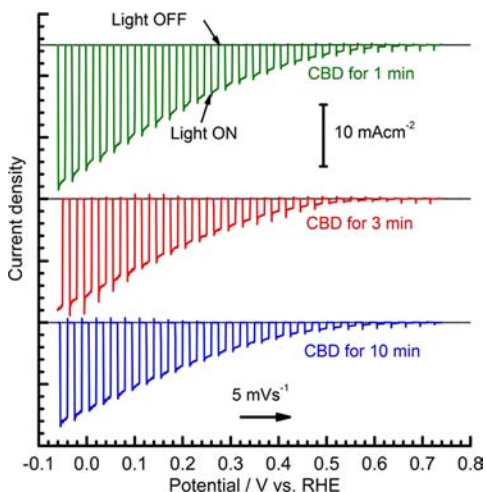


**Figure 2.** Current–potential curves for Pt/CdS/CGSe electrodes obtained using different CBD times [0.1 M Na<sub>2</sub>SO<sub>4</sub>(aq), pH 9, 300 W Xe lamp, 5 mV s<sup>-1</sup>].

prepared with different CBD times. The photocurrent was highest for a deposition time of 1 min. The solar energy conversion efficiency under simulated solar irradiation (AM1.5G) for the 1 min CBD sample was found to be 0.83% at 0.2 V vs RHE<sup>11</sup> (see the SI). However, this result was contradictory because a thicker CdS layer can form a thicker depletion layer, which may be preferable for charge separation.

The wavelength dependence of the incident photon to current conversion efficiency (IPCE) for Pt/CdS/CGSe electrodes with CBD times of 1 and 10 min are shown in Figure 3. The IPCEs were measured at 0 V vs RHE, and the sample was irradiated with monochromatic light using a 300 W

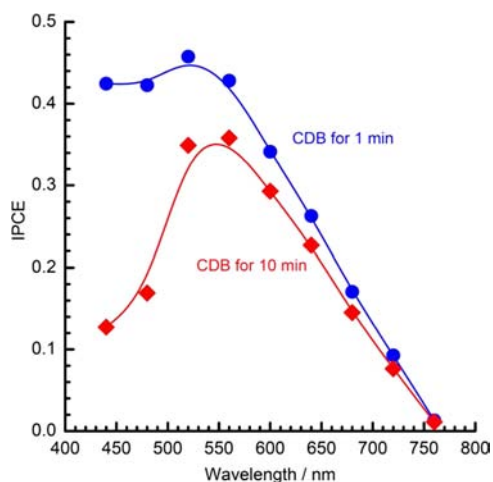


**Figure 3.** Wavelength dependence of the IPCEs for Pt/CdS/CGSe electrodes with different CdS layer thicknesses [0.1 M Na<sub>2</sub>SO<sub>4</sub> (aq), pH 9, 300 W Xe lamp, 0 V vs RHE].

Xe lamp equipped with a band-pass filter and an optical fiber. The photon flux was determined using a calibrated Si photodiode. The Pt/CdS/CGSe electrode obtained by CBD for 1 min showed a higher IPCE than the 10 min CBD sample at all wavelengths. However, at wavelengths shorter than 500 nm (the absorption edge of CdS), 10 min CBD sample had a much lower efficiency than the 1 min CBD sample. Therefore, photons absorbed by CdS were forced to recombine. One possible reason for the noticeable efficiency loss at  $\lambda < 500$  nm is the recombination of photocarriers generated in the CdS layer despite the existence of band bending due to the poor crystal quality. The difference in IPCE at  $\lambda > 500$  nm is likely due to the difference in the quality of the CdS–CGSe interface. During CBD of the CdS layer, Cd diffuses into the CGSe, and the CGSe becomes an n-type material as a result of Cd doping.<sup>12</sup> The decrease in IPCE with increasing CBD time is likely due to degradation of the p-type semiconducting properties of the CGSe as a result of Cd diffusion.

Calculated band alignments at the solid–electrolyte interfaces of CGSe and CdS/CGSe electrodes are shown in Figure 4. The difference between the Fermi level ( $E_F$ ) and the VBM of

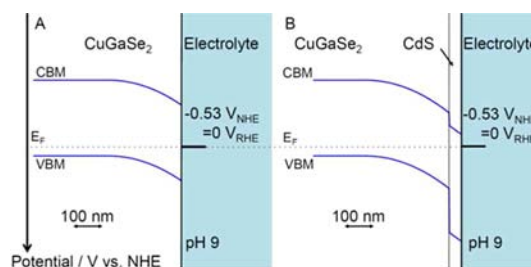


**Figure 4.** Calculated band alignment at the solid–electrolyte interfaces for (A) CGSe and (B) CdS/CGSe electrodes.

CGSe and that between  $E_F$  and the CBM of CdS were assumed to be 0.2 eV. The flat-band potentials of CGSe and CdS are 0.55 V (see the SI) and  $-0.1$  V vs RHE at pH 9, respectively.<sup>13</sup> The CBM offset between CGSe and CdS was reported to be 0.28 eV.<sup>14</sup> Under the supposition of a carrier concentration of  $10^{16}$  cm<sup>-3</sup> for both CGSe and CdS, the thickness of the depletion layers formed at the solid–electrolyte interface would be 250 and 320 nm for CGSe and CdS/CGSe, respectively.

One possible reason for the increased photocurrent and onset potential is the increased thickness of the depletion layer formed at the solid–electrolyte interface, which plays a principal role in charge separation. Another possible reason is selective diffusion of electrons into “charge vacant” CdS layers due to the VBM offset between CGSe and CdS (0.98 eV).

To examine the durability of Pt/CdS/CGSe, the time course of the photocurrent was measured. Figure 5 shows a current–

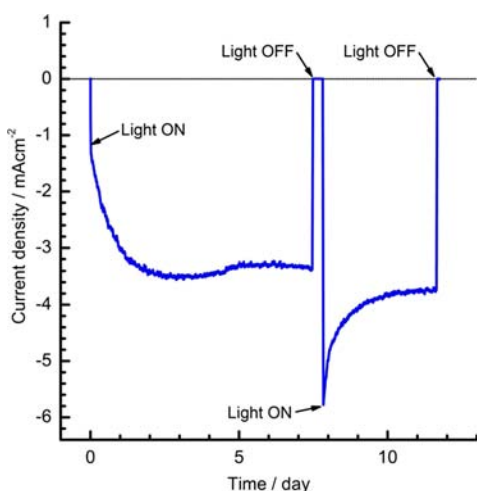


**Figure 5.** Current–time curve for a Pt/CdS/CuGaSe<sub>2</sub> electrode [0.05 M Na<sub>2</sub>HPO<sub>4</sub>(aq) + 0.05 M NaH<sub>2</sub>PO<sub>4</sub>(aq), pH 7, 150 W Xe lamp, 0 V vs RHE].

time curve for a Pt/CdS/CGSe electrode at a potential of 0 V vs RHE. A stability test was performed in a phosphate buffer to avoid any change in pH. The CdS layer was formed by CBD for 3 min. Stabilization of the photocathodic current was eventually achieved after 2 days. We note that the contribution of the cathodic photocurrent to the hydrogen evolution was confirmed (see the SI). Hydrogen evolved steadily for more than 1 week. We note that the *I*–*E* curve for the sample changed after the stability test, and the photocurrent in the sample increased. SEM images of the sample indicated that some of the CdS dissolved in the solution, but the surface remained fully covered with CdS, as confirmed by XPS (see the SI). Therefore, the photocurrent in the sample may have increased because the CdS layer became thinner. One of the reasons for the photocurrent stability is protection of the bulk of the photoelectrodes by the existence of partially reduced CdS layers, as found in the XPS results.

In summary, a CuGaSe<sub>2</sub> photoelectrode was prepared by coevaporation and modified by CdS CBD. The conduction-band minimum and valence-band maximum for the CuGaSe<sub>2</sub> were –0.8 and +0.9 V vs NHE, respectively. CdS deposition greatly increased the photocurrent in the CuGaSe<sub>2</sub> photocathode, and the optimal deposition time was 1 min. This might be due to charge separation caused by the surface p–n junction with appropriate band alignment and photon absorption by the CdS, which was not used for water reduction. A Pt/CdS/CuGaSe<sub>2</sub> electrode generated a stable photocurrent under reductive conditions for more than 10 days under visible-light irradiation. It can be concluded that CuGaSe<sub>2</sub> is a promising material for practical use in photoelectrochemical water splitting, although further investigation is required.

## ■ ASSOCIATED CONTENT

### ■ Supporting Information

Preparation of CuGaSe<sub>2</sub> films on Mo-coated soda lime glass plates by coevaporation method, CBD of CdS, electrode preparation for PEC measurements, results of PEC measurements, calculation of band alignment at the electrode–electrolyte interface, results of sample analysis, *I*–*E* curve under simulated sunlight, cross-sectional SEM–EDS mapping, Mott–Schottky plot for a prepared CuGaSe<sub>2</sub> electrode, XPS and SEM results before and after the durability test, and results of gas product analysis. This material is available free of charge via the Internet at <http://pubs.acs.org>.

## ■ AUTHOR INFORMATION

### Corresponding Author

domen@chemsys.t.u-tokyo.ac.jp

### Notes

The authors declare no competing financial interest.

## ■ ACKNOWLEDGMENTS

This work was supported in part by a Grant-in-Aid for Specially Promoted Research (23000009) from the Japan Society for the Promotion of Science (JSPS) and the Advanced Low Carbon Technology Research and Development Program (ALCA) of the Japan Science and Technology Agency (JST). This work also contributes to the international exchange program of the A3 Foresight Program of JSPS.

## ■ REFERENCES

- (1) Walter, M. G.; Warren, E. L.; McKone, J. R.; Boettcher, S. W.; Mi, Q.; Santori, E. A.; Lewis, N. S. *Chem. Rev.* **2010**, *110*, 6446–6473.
- (2) Hernandez-Rojas, J.; Jucia, M.; Martil, I.; Gonzalez-Diaz, G.; Santamaria, J.; Sanchez-Quesada, F. *Appl. Opt.* **1992**, *31*, 1606–1611.
- (3) Marsen, B.; Cole, B.; Miller, E. L. *Sol. Energy Mater. Sol. Cells* **2008**, *92*, 1054–1058.
- (4) Yokoyama, D.; Minegishi, T.; Maeda, K.; Katayama, M.; Kubota, J.; Yamada, A.; Konagai, M.; Domen, K. *Electrochem. Commun.* **2010**, *12*, 851–853.
- (5) Jiang, C.-S.; Hasoon, F. S.; Moutinho, H. R.; Al-Thani, H. A.; Romero, M. J.; Al-Jassim, M. M. *Appl. Phys. Lett.* **2003**, *82*, 127–129.
- (6) Kim, J.; Minegishi, T.; Kubota, J.; Domen, K. *Energy Environ. Sci.* **2012**, *5*, 6368–6374.
- (7) Kim, J.; Minegishi, T.; Kubota, J.; Domen, K. *Jpn. J. Appl. Phys.* **2012**, *51*, No. 015802.
- (8) Yokoyama, D.; Minegishi, T.; Jimbo, K.; Hisatomi, T.; Ma, G.; Katayama, M.; Kubota, J.; Katagiri, H.; Domen, K. *Appl. Phys. Express* **2010**, *3*, No. 101202.
- (9) Lu, X.; Minegishi, T.; Kubota, J.; Domen, K. *Jpn. J. Appl. Phys.* **2011**, *50*, No. 085702.
- (10) ICDD no. 31-0456.
- (11) Chen, Z.; Jaramillo, T.; Deutsch, T.; Kleiman-Shwarsstein, A.; Forman, A.; Gaillard, N.; Garland, R.; Takanabe, K.; Heske, C.; Sunkara, M.; McFarland, E.; Domen, K.; Miller, E.; Turner, J.; Dinh, H. *J. Mater. Res.* **2010**, *25*, 3–16.
- (12) Fons, P.; Sakurai, K.; Yamada, A.; Matsubara, K.; Iwata, K.; Baba, T.; Kimura, Y.; Nakanishi, H.; Niki, S. *J. Phys. Chem. Solids* **2003**, *64*, 1733–1735.
- (13) Watanabe, T.; Fujishima, A.; Honda, K. *Chem. Lett.* **1974**, 897–900.
- (14) Schulmeyer, T.; Kniese, R.; Hunger, R.; Jaegermann, W.; Powalla, M.; Klein, A. *Thin Solid Films* **2004**, 451–452, 420–423.